Title

Abnormal white matter microstructure in children with sensory processing disorders.

Authors

Desai, Shivani
Fourie, Emily
Harris, Julia
et al.

Publication Date

2013

DOI

10.1016/j.nicl.2013.06.009

NeuroImage: Clinical 2 (2013) 844–853

Contents lists available at ScienceDirect

NeuroImage: Clinical

journal homepage: www.elsevier.com/locate/ynicl

Abnormal white matter microstructure in children with sensory processing disorders ☆

Julia P. Owen [a,b,1], Elysa J. Marco [c,1], Shivani Desai [c], Emily Fourie [a], Julia Harris [c], Susanna S. Hill [c], Anne B. Arnett [d], Pratik Mukherjee [a,b,*]

[a] Department of Radiology and Biomedical Imaging, University of California, San Francisco, 185 Berry Street, San Francisco, CA 94107, USA
[b] Program in Bioengineering, University of California, San Francisco, 1700 4th St., San Francisco, CA 94158, USA
[c] Department of Neurology, University of California, San Francisco, 675 Nelson Rising Lane, San Francisco, CA 94158, USA
[d] Department of Psychology, University of Denver, Frontier Hall, 2155 S. Race Street, Denver, CO 80208, USA

ARTICLE INFO

Article history:
Received 26 March 2013
Received in revised form 2 June 2013
Accepted 17 June 2013
Available online 23 June 2013

Keywords:
Attention deficit hyperactivity disorder (ADHD)
Autism
Brain development
Connectivity
Diffusion tensor imaging (DTI)
Pediatrics

ABSTRACT

Sensory processing disorders (SPD) affect 5–16% of school-aged children and can cause long-term deficits in intellectual and social development. Current theories of SPD implicate primary sensory cortical areas and higher-order multisensory integration (MSI) cortical regions. We investigate the role of white matter microstructural abnormalities in SPD using diffusion tensor imaging (DTI). DTI was acquired in 16 boys, 8–11 years old, with SPD and 24 age-, gender-, handedness- and IQ-matched neurotypical controls. Behavior was characterized using a parent report sensory behavior measure, the Sensory Profile. Fractional anisotropy (FA), mean diffusivity (MD) and radial diffusivity (RD) were calculated. Tract-based spatial statistics were used to detect significant group differences in white matter integrity and to determine if microstructural parameters were significantly correlated with behavioral measures. Significant decreases in FA and increases in MD and RD were found in the SPD cohort compared to controls, primarily involving posterior white matter including the posterior corpus callosum, posterior corona radiata and posterior thalamic radiations. Strong positive correlations were observed between FA of these posterior tracts and auditory, multisensory, and inattention scores ($r = 0.51–0.78$; $p < 0.001$) with strong negative correlations between RD and multisensory and inattention scores ($r = -0.61–0.71$; $p < 0.001$). To our knowledge, this is the first study to demonstrate reduced white matter microstructural integrity in children with SPD. We find that the disrupted white matter microstructure predominantly involves posterior cerebral tracts and correlates strongly with atypical unimodal and multisensory integration behavior. These findings suggest abnormal white matter as a biological basis for SPD and may also distinguish SPD from overlapping clinical conditions such as autism and attention deficit hyperactivity disorder.

1. Introduction

Sensory processing disorders (SPD) affect 5–16% of children and can cause long-term impairment of intellectual and social development from disrupted processing and integration of high-bandwidth information from multiple sensory modalities simultaneously (Ahn et al., 2004; Ben-Sasson et al., 2009a; Brett-Green et al., 2008; Bundy et al., 2007). There is co-morbidity with attention deficit hyperactivity disorder (ADHD), autism and other psychopathology, but SPD often exists in isolation (Ahn et al., 2004; Ben-Sasson et al., 2009b; Leekam et al., 2007; Van Hulle et al., 2012). Sensory dysregulation is also prevalent in children born prematurely and those with fragile X syndrome (Baranek et al., 2008; Goldsmith et al., 2006; Wickremasinghe et al., 2013). While there have been many prior investigations of the biological basis of ADHD, autism, prematurity, and even less common diseases such as fragile X, the neural substrates of SPD remain poorly understood.

Current hypotheses regarding the underlying basis of SPD implicate both primary sensory cortical areas and higher-order cortical regions subserving multimodal sensory integration (MSI). Specifically, the posterior parietal cortex and superior temporal sulcus are involved in auditory–tactile integration, whereas dorsolateral prefrontal cortex helps mediate attentional control (Brett-Green et al., 2008; Chait et al., 2010). Prior studies of SPD have focused on neurophysiological methods such as electroencephalography to define the neural origins

* Corresponding author at: Center for Molecular and Functional Imaging, Department of Radiology and Biomedical Imaging, University of California, San Francisco, UCSF Box 0946, 185 Berry Street, Suite 350, San Francisco, CA 94107, USA. Tel.: +1 415 514 8186; fax: +1 415 353 8593.
E-mail address: pratik.mukherjee@ucsf.edu (P. Mukherjee).

[1] These authors contributed equally to the paper.

2213-1582/$ – see front matter © 2013 The Authors. Published by Elsevier Inc. All rights reserved.
http://dx.doi.org/10.1016/j.nicl.2013.06.009

of sensory processing deficits (Brett-Green et al., 2008, 2010). However, the role of white matter in SPD has not, to our knowledge, been previously investigated.

Microstructural characteristics of white matter tracts, such as axonal diameter, fiber density and myelination are crucial for determining the speed and bandwidth of information transmission in the human brain. Microstructural abnormalities of fibers in primary sensory tracts and/or in tracts connecting multimodal association areas may result in loss of the precise timing of action potential propagation needed to accomplish accurate sensory processing and MSI. The advent of diffusion tensor imaging (DTI) has enabled the noninvasive evaluation of white matter microstructure (Basser et al., 1994; Mori et al., 1999; Mukherjee et al., 2008).

Fractional anisotropy (FA) values from DTI represent the orientation-dependent variation of water diffusivity and reflect microstructural properties such as axon diameter, degree of myelination, fiber packing density and fiber collimation (Beaulieu, 2002; Mukherjee et al., 2008). Mean diffusivity (MD) is the rate of diffusion averaged over all orientations. Axial diffusivity (AD) is the rate of diffusion along the orientation of white matter fibers within a tract, whereas radial diffusivity (RD) is the rate of diffusion orthogonal to the fiber orientation. Normal white matter maturation during childhood produces increasing FA, decreasing MD and decreasing RD, with relatively smaller changes in AD (Mukherjee and McKinstry, 2006; Mukherjee et al., 2001, 2002; Yoshida et al., 2013). Conversely, white matter pathology typically causes decreased FA, elevated MD and elevated RD, collectively referred to as reduced "microstructural integrity".

We hypothesize that, compared to typically developing children (TDC), children with SPD will have reduced white matter microstructural integrity, particularly not only in primary sensory projection pathways, but also in association pathways and commissural connections which facilitate higher-order sensory processing and MSI. Furthermore, we hypothesize that DTI metrics of white matter microstructure such as FA will correlate with behavioral measures of sensory processing function and MSI in both the SPD and TDC groups.

2. Methods

2.1. Demographic, sensory, cognitive and behavioral data

2.1.1. General demographics and sensory, cognitive and behavioral assessment

Sixteen right-handed males with SPD and 24 right-handed male TDCs, all between 8 and 11 years of age, were prospectively enrolled under our institutional review board approved protocol. Subjects were recruited from the Autism & Neurodevelopment Program and from local online parent board listings. Informed consent was obtained from the parents or legal guardians, with the assent of all participants.

All subjects were assessed with the Wechsler Intelligence Scale for Children-Fourth Edition (Wechsler, 2003) and the Sensory Profile (Dunn and Westman, 1997). The Sensory Profile is a parent report questionnaire which measures behavioral sensory differences, yielding scores within individual sensory domains and factors and a total score. A probable difference in sensory behavior is defined as a total score from 142 to 154, while a definite difference corresponds to a total score of $\leq$141. We used the auditory, visual, tactile, multisensory and inattention scores to explore behavioral correlations.

2.1.2. Autistic spectrum disorder (ASD)

Three of the boys with SPD, but none of the typically developing children, had abnormally high scores on the social communication questionnaire (SCQ), a parent report screening test for ASD (Eaves et al., 2006). The parents of these three subjects were further administered the full Autism Diagnostic Inventory-Revised (ADIR) (Lord et al., 1994) and the three children themselves were tested with the Autism Diagnostic Observation Schedule (ADOS) (Lord et al., 1989). One of the boys scored in the range of ASD on the ADOS and another was found to be in the ASD range on the ADIR, but none met the criteria for ASD on both exams. Evaluation of these three subjects by Dr. Marco, a child neurologist experienced in autism, was also not consistent with an ASD diagnosis.

2.1.3. Attention deficits

On the inattention measure of the Sensory Profile, eleven of the 16 SPD subjects scored in the definite difference range, four in the probable difference range, and one in the typical range. Of the 24 typically developing children, none scored in the definite difference range, four in the probable difference range, and twenty in the typical range.

2.1.4. Prematurity

Three of 16 SPD boys were born prematurely, one at 32 weeks gestation and two at 34 weeks gestation. One of the 24 typically developing children was born prematurely, at 33 weeks gestation. These four subjects were found to be in the middle of the distribution for global FA and mean FA extracted from clusters of significantly affected voxels (described below) for their respective groups; hence, they did not represent outliers.

2.2. Image acquisition

MR imaging was performed on a 3 T Tim Trio scanner (Siemens, Erlangen, Germany) using a 12-channel head coil. Structural MR imaging of the brain was performed with an axial 3D magnetization prepared rapid acquisition gradient-echo T1-weighted sequence (TE = 2.98 ms, TR = 2300 ms, TI = 900 ms, flip angle of 9°) with a 256 mm field of view (FOV), and 160 1.0 mm contiguous partitions at a 256 × 256 matrix. Whole-brain DTI was performed with a multislice 2D single-shot twice-refocused spin-echo echo-planar sequence with 64 diffusion-encoding directions, diffusion-weighting strength of $b = 2000$ s/mm^2, iPAT reduction factor of 2, TE/TR = 109/8000 ms, NEX = 1, interleaved 2.2 mm axial slices with no gap, and in-plane resolution of 2.2 × 2.2 mm with a 100 × 100 matrix and FOV of 220 mm. An additional image volume was acquired with no diffusion weighting ($b = 0$ s/mm^2). The total DTI acquisition time was 8.67 min.

2.3. DTI analysis

2.3.1. Pre-processing

The diffusion-weighted images were corrected for motion and eddy currents using FMRIB's Linear Image Registration Tool (FLIRT; www.fmrib.ox.ac.uk/fsl/flirt) with 12-parameter linear image registration (Jenkinson et al., 2002). All diffusion-weighted volumes were registered to the reference $b = 0$ s/mm^2 volume. To evaluate subject movement, we calculated a scalar parameter quantifying the transformation of each diffusion volume to the reference. A heteroscedastic two-sample Student's t-test verified that there were no significant differences between SPD and TDC groups in movement during the DTI scan ($p > 0.05$). The non-brain tissue was removed using the Brain Extraction Tool (BET; http://www.fmrib.ox.ac.uk/analysis/research/bet). FA, MD, AD and RD were calculated using FSL's DTIFIT.

2.3.2. Tract-based spatial statistics

Using Tract-Based Spatial Statistics (TBSS) in FSL (Smith et al., 2006), FA maps from all 40 boys were aligned to the FA map of the "most representative subject". This procedure is recommended for children because the standard FA template is derived from adults. Once all subjects were registered, the FA maps were thinned using FA > 0.2 to create a skeleton of the white matter. Then, skeletonized MD, AD, and RD maps were created. Two contrasts for each DTI parameter were used to assess for group differences with nonparametric permutation testing via the "randomise" function in FSL: SPD > TDC and TDC > SPD.

The resulting group difference maps for each comparison were corrected for multiple comparisons over the 3D image volume with threshold-free cluster enhancement (TFCE) (Smith and Nichols, 2009), using a significance threshold of $p < 0.05$. It is important to note that, in TFCE, the cluster, and not the individual voxel, is the ultimate object of statistical inference and therefore every voxel in the cluster has exactly the same level of statistical significance in the final results.

The anatomic locations of white matter regions corresponding to statistically significant clusters of voxels were determined from the Johns Hopkins University (JHU) ICBM-DTI-81 White-Matter Labeled Atlas and the JHU White-Matter Tractography Atlas, both are available for MNI152 space in FSL (Mori et al., 2005, 2008). All white matter region identifications were verified by Dr. Mukherjee, a board-certified pediatric neuroradiologist with over 15 years of experience in clinical and research applications of DTI.

2.3.3. Correlation of DTI with sensory processing measures

The auditory, tactile, visual, multisensory, and inattention scores for TDC and SPD subjects were mean-centered across all subjects. The DTI parameters were also demeaned. Two contrasts were used for each pair of cognitive variable and DTI parameter to test for correlation and anti-correlation at the cluster level. As with the group difference analysis, the maps for each contrast were corrected for multiple comparisons with TFCE and thresholded for significance at $p < 0.05$. For the maps with statistically significant clusters of voxels, we extracted the largest 3 or 4 clusters from the thresholded image and calculated the mean across voxels of each DTI parameter in each cluster. Then we computed the Pearson's correlation coefficient and associated p-value for the mean DTI parameter in the cluster versus the sensory variable.

2.4. Morphometric image analysis

The 3D T1-weighted image volume for each subject was automatically segmented using FreeSurfer 5.1.0 (Fischl, 2012). The right and left cerebral hemisphere white matter and gray matter volumes, and supratentorial and intracranial volumes, were computed. A heteroscedastic two-sample Student's t-test was performed for each of these volumes to evaluate for group differences between TDC and SPD.

3. Results

3.1. Assessment of sensory, cognitive and behavioral functioning

There were no significant differences between SPD and TDC groups in age or IQ (Table 1). Four SPD subjects displayed probable difference according to the total score of the Sensory Profile, while twelve showed definite difference. All four SPD boys in the probable difference range had auditory scores in the definite difference range. All TDC subjects had total scores of ≥ 158, which fall in the typical range. As expected, the SPD group was worse than the TDC group on all Sensory Profile measures (Table 1). Principal component analysis demonstrated that these Sensory Profile measures were highly correlated. The first principal component accounted for 80% of the variance in the data and received approximately equal weighting from all five measures (Fig. 1). The SPD group also showed significantly greater deficits than controls on the social communication questionnaire (SCQ in Table 1); however, none of the SPD participants met the diagnostic criteria for autism.

3.2. MRI structural and morphometric analysis

Structural brain MR imaging assessed by a board-certified pediatric neuroradiologist, Dr. Mukherjee, revealed normal findings in all participants, except for an incidental arachnoid cyst adjacent to the left cerebellum in one SPD subject. This subject was not excluded because the cyst did not affect DTI image registration and the subject was not an outlier for either DTI measurements or sensory, cognitive or behavioral assessments compared to the rest of the SPD cohort.

Table 1
Demographic information and sensory profile subscores.

Sensory score	TDC (mean ± std dev)	SPD (mean ± std dev)	p-Value
Age (years)	9.9 ± 1.0	9.7 ± 1.3	P = 0.65
FSIQ	115 ± 9	113 ± 10	P = 0.63
VIQ	119 ± 12	117 ± 13	P = 0.66
PIQ	114 ± 13	116 ± 12	P = 0.63
SCQ	2.2 ± 2.1	9.6 ± 7.2	P < 0.001
Auditory	33.5 ± 3.5	22.7 ± 4.9	p < 0.00001
Tactile	83.3 ± 5.7	62.9 ± 8.8	p < 0.00001
Visual	41.0 ± 3.0	32.3 ± 7.1	p < 0.00001
Multisensory	31.3 ± 3.0	22.4 ± 4.8	p < 0.00001
Inattention	28.6 ± 3.5	17.8 ± 5.3	p < 0.00001

FSIQ — full scale intelligence quotient.
PIQ — performance intelligence quotient.
SCQ — social communication questionnaire.
SPD — sensory processing disorders.
TDC — typically developing children.
VIQ — verbal intelligence quotient.

There were no significant group differences in global or regional brain volumes between SPD and TDC from the FreeSurfer analysis: left cerebral white matter ($p = 0.46$), right cerebral white matter ($p = 0.33$), left cerebral cortical volume ($p = 0.94$), right cerebral cortical volume ($p = 0.82$), total supratentorial volume ($p = 0.57$), and total intracranial volume ($p = 0.53$).

3.3. Group differences: DTI parameters

Significant differences ($p < 0.05$) in FA, MD, and RD were detected between the TDC and SPD boys after correction for multiple comparisons (Fig. 2). There were decreases of FA in SPD subjects versus controls in the posterior body and isthmus of the corpus callosum, the left posterior thalamic radiations (PTR), left posterior corona radiata (PCR), and the posterior aspect of the left superior longitudinal fasciculus (SLF). Regions of the right PTR and right PCR also demonstrated strong trends toward decreased FA ($p < 0.055$) in SPD.

White matter tracts with significant differences in MD and RD between SPD and TDC were similar to those for FA. Increases of MD and RD in SPD versus controls ($p < 0.05$) were present in bilateral PTR, SLF and posterior corpus callosum. RD showed more extensive regions of abnormal white matter in SPD than either FA or MD, with significantly reduced RD extending to the splenium of the corpus callosum and to frontal tracts such as the left anterior thalamic radiations (ATR), the left anterior corona radiata (ACR), and the left forceps minor. There was no white matter region in which AD was significantly different between the groups.

3.4. Correlation analysis: DTI parameters versus behavioral measures

Significant positive correlations ($p < 0.05$) were detected between FA and the auditory, multisensory, and inattention scores across both SPD and TDC groups. Significant negative correlations were detected between RD and the multisensory and inattention scores of both groups. These results show that more typical behavior is associated with higher FA and lower RD.

Three significant clusters were extracted from correlation of FA with the auditory score: left and right PTR and the posterior body and isthmus of the corpus callosum (Fig. 3). For MSI, there were three clusters where FA showed positive correlation and three clusters where RD showed negative correlations (Fig. 4). Strong positive correlations of FA with multisensory score were observed in the posterior body, isthmus and splenium of the corpus callosum and in right

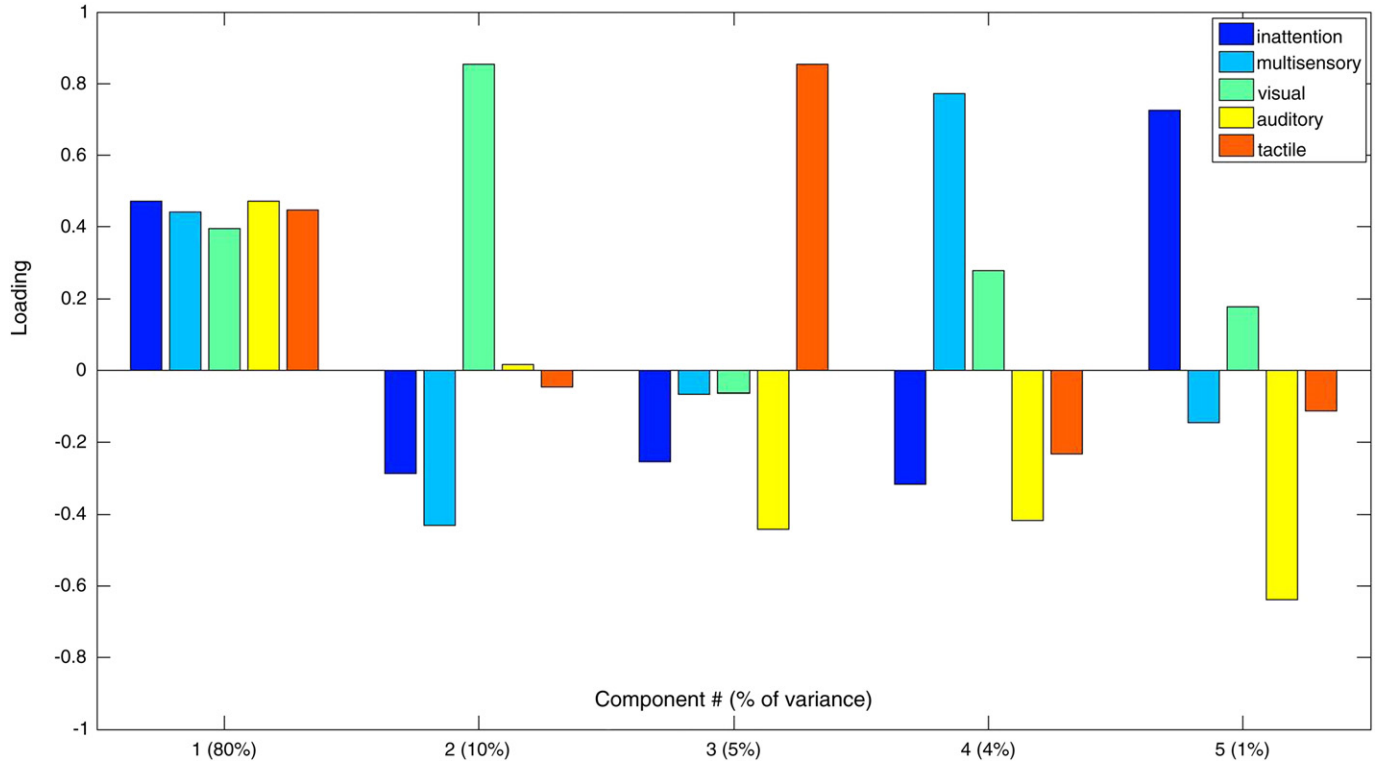

Fig. 1. Principal component analysis of Sensory Profile scores in SPD subjects and matched controls.

PCR and bilateral SLF. Strong negative correlations of RD with multisensory score were found in the left PTR, right PCR, and left SLF.

For the inattention score, four clusters were identified where FA exhibited positive correlation and three clusters were found where RD exhibited negative correlations (Fig. 5). Similar to the findings with auditory and multisensory scores, positive correlation of FA with inattention score was discovered in both left and right PCR and PTR, left SLF and throughout the posterior corpus callosum. Comparable regions in bilateral PTR and PCR were found where RD is negatively correlated with inattention score. However, specific to the inattention score is a cluster in the left ACR and ATR (Fig. 5E) where FA is positively correlated and a cluster in the left SLF (Fig. 5D) where RD is negatively correlated.

After correction for multiple comparisons over the whole brain, there were no clusters identified where AD or MD were significantly correlated with auditory, multisensory, or inattention scores. Although no DTI correlations with visual or tactile domain scores survived multiple comparison correction, hypothesis-driven region of interest measurements of FA do show significant correlations with visual and tactile scores in the same regions of the left and right PTR that are significantly correlated with auditory scores (Fig. 6). There is also a strong trend toward significance in the correlation of FA with visual and tactile scores in the same region of the posterior corpus callosum that is significantly correlated with auditory scores.

4. Discussion

4.1. Abnormal white matter microstructure in sensory processing disorders

To our knowledge, this is the first study to demonstrate abnormal white matter microstructure in children with SPD. The strength of our methodology is automated data-driven detection of group differences in white matter microstructure over the entire brain using TBSS. The results support our a priori hypothesis that the most affected tracts would be primary sensory cerebral tracts and pathways connecting higher-order and multimodal sensory regions where MSI takes place. Excluding olfaction, the central primary sensory projection pathways are all contained within the PTR of both hemispheres, including the somatosensory radiations, acoustic radiations and optic radiations. Homologous sensory cortical regions of the left and right cerebral hemispheres are connected via commissural fibers of the posterior corpus callosum, including the posterior body, isthmus and splenium (Hofer and Frahm, 2006; Huang et al., 2005). These posteriorly located projection and commissural tracts are precisely where the greatest reductions in microstructural integrity were seen in the SPD cohort relative to controls (Fig. 2). No brain volumetric differences were found between SPD and TDC cohorts in gray or white matter, indicating that the pathology is not primarily at the macrostructural scale.

These imaging observations suggest that white matter microstructure is a biological substrate for the atypical sensory behaviors of children with SPD and also help to establish SPD as a clinical entity distinct from overlapping conditions such as autism spectrum disorders and ADHD. ASD and ADHD have been reported to show primarily frontotemporal patterns of abnormality on DTI (Tamm et al., 2012; Travers et al., 2012). In ADHD, the most consistent findings have been abnormal FA in tracts with prefrontal connectivity, including SLF, ACR and fronto-striatal pathways (Liston et al., 2011; Tamm et al., 2012). Reduced white matter microstructural integrity in ASD can be widespread, but has been more commonly found in frontal and temporal tracts (Travers et al., 2012), rather than the predominantly parietal and occipital tracts shown in our study of SPD.

4.2. Correlation of white matter microstructure with atypical sensory behaviors and inattention

Another advantage of our methodology is the use of TBSS to detect correlations of white matter microstructure with measures of sensory behavior, MSI and attention derived from the Sensory Profile. This automated whole-brain analysis revealed significant correlations of DTI parameters with auditory and multisensory scores in the same posterior projection and commissural tracts that were found to be

abnormal in the group comparison of SPD vs TDC. These results bolster our hypothesis that DTI metrics of white matter microstructure are relevant to the atypical sensory behaviors that form the clinical core of this disorder. R^2 values derived from the correlation coefficients suggest that one-third to one-half of the variance in auditory and multisensory scores can be explained by FA of the PTR, whereas one-quarter can be explained by FA of the posterior corpus callosum.

Correlations were sought between DTI microstructural parameters and Sensory Profile scores across both groups of subjects, which assumes that every subject lies on a continuum regardless of group membership. After correction for multiple comparisons, significant correlations were found in predominantly posterior white matter tracts, with little overlap between the two groups along the regression lines. It is not surprising that there is little overlap between the SPD and TDC groups for the auditory and multisensory scores (Figs. 3–4, Table 1), since those scores were used to diagnose SPD. The interesting discovery is that DTI microstructural parameters closely correlate with these Sensory Profile scores in those central white matter pathways known to be involved in primary sensory information transmission, such as the PTR, and in connectivity between cortical regions subserving unimodal and multimodal sensory processing, such as the posterior corpus callosum. Therefore, DTI metrics in those tracts also separate the two groups effectively. The extent of variation of DTI metrics and Sensory Profile scores in the two groups also supports the hypothesis that sensory processing is a spectrum disorder, with a range of performance across both TDC and SPD groups.

Given the strong co-linearity among the five measures of the Sensory Profile (Fig. 1), associations between the microstructure of central sensory tracts and parental sensory ratings were not modality-specific. Instead, cross-modality correlations were often found, such as between FA of the optic radiations and auditory score. Correlations of FA and RD with the inattention score not only showed significant clusters similar to those of auditory and MSI scores, such as the bilateral PTR and the posterior corpus

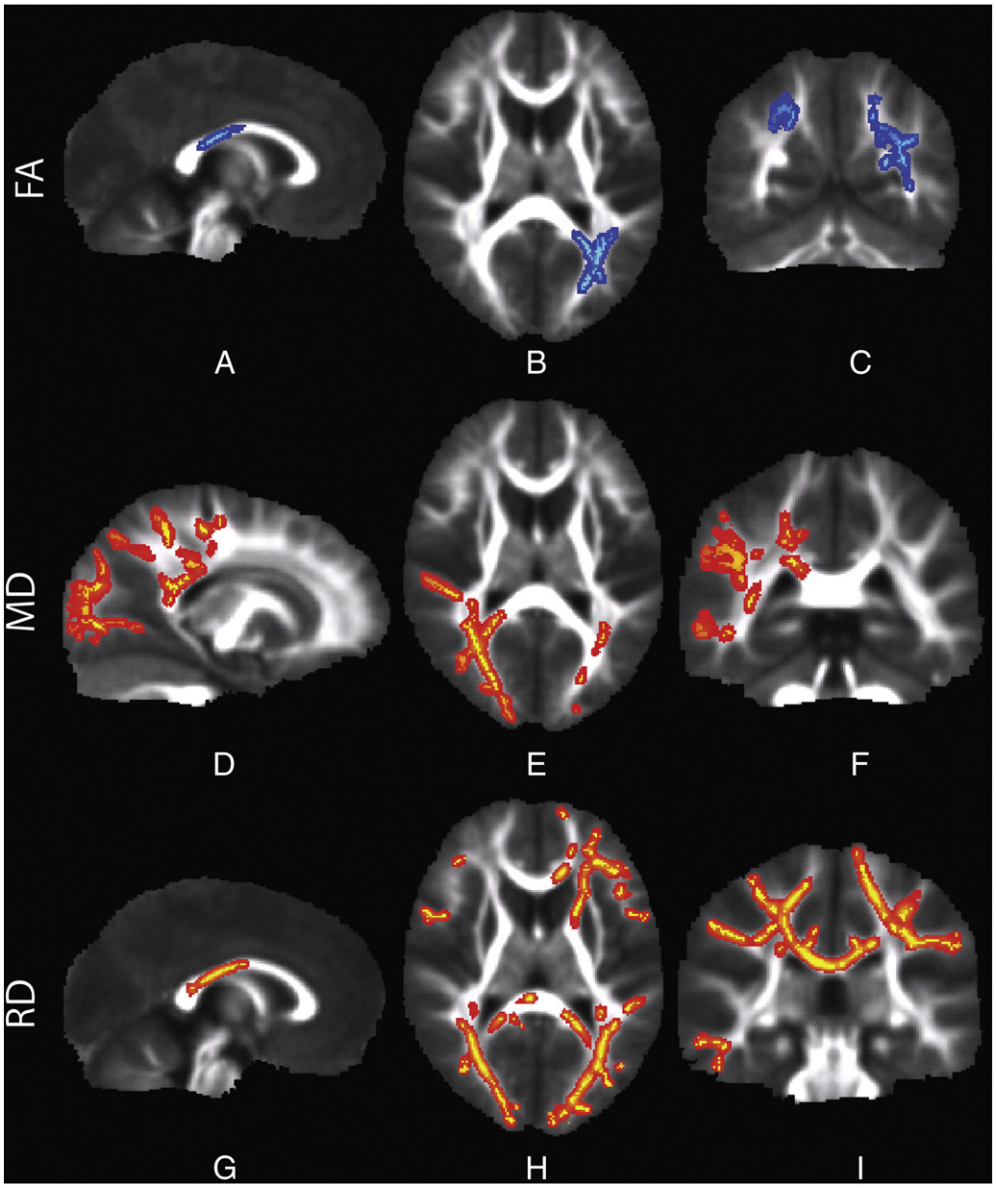

Fig. 2. A–C demonstrates reduced FA in SPD in the posterior body of the corpus callosum and bilateral PTR. D–F demonstrates increased MD in the SPD patients in the lateral callosal fibers of the posterior body and splenium, bilateral PTR, including the optic radiations, right PCR, and right SLF. G–I shows increased RD in the posterior body and splenium, bilateral PTR, including the optic radiations, left ATR, and left forceps minor. The color scheme denotes TDC > SPD in blue and SPD > TDC in red and all images are presented in radiological convention (left hemisphere on right side of image).

callosum, but also showed involvement of some frontal tracts, greater on the left than right. This likely reflects prefrontal contributions to attentional function that are not present with primary sensory processing.

4.3. Limitations and future directions

This exploratory investigation of white matter microstructure in SPD is limited by small sample size and needs to be replicated in larger cohorts. To increase the homogeneity of these groups of SPD and TDC subjects, the study was restricted to boys, aged 8–11 years, with normal IQ. Therefore, further research is needed to determine whether the findings generalize to other ages, both genders and the full spectrum of intellectual ability. Another limitation is that assessments of sensory processing, MSI and inattention were based on the Sensory Profile, a parent questionnaire with measures that show strong co-linearity (Fig. 1). This can be addressed in future studies that incorporate objective tests of sensory processing that may be more specific to each sensory modality. Correlations of white matter microstructure with tactile and visual processing were weaker than with auditory processing (Figs. 3, 6) and did not survive whole-brain multiple comparisons correction in this small cohort. This may be because all 16 SPD boys showed definite differences in the auditory domain, but only 12 showed definite differences on the

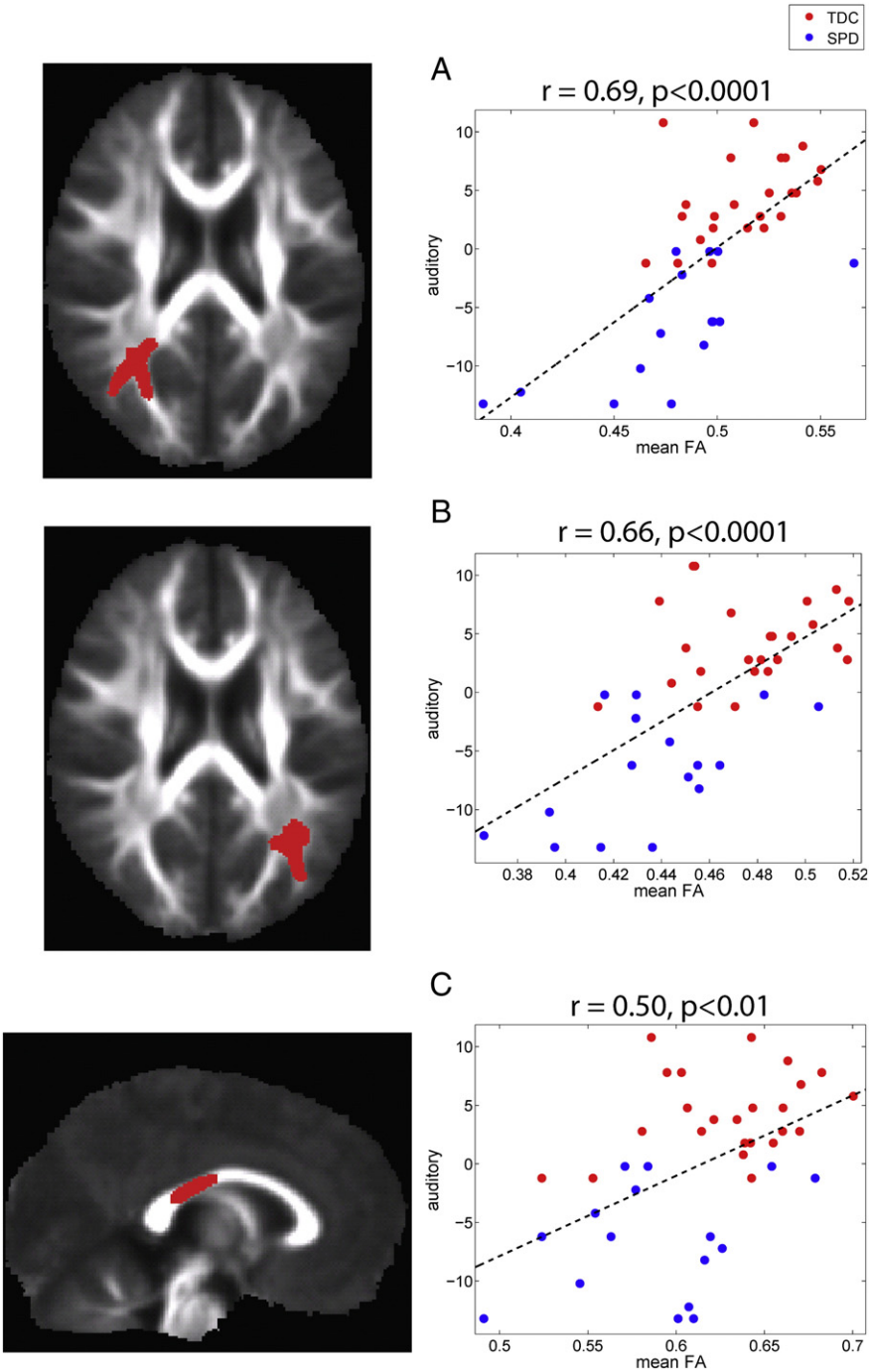

Fig. 3. Correlation of FA with auditory sensory score: The left column displays the clusters extracted from the statistical image for the correlation ($p < 0.05$) and the right column displays the plot of mean FA in each cluster versus the mean-centered auditory score for the TDC (red) and SPD (blue) groups. The correlation coefficient and corresponding p-value are provided for each cluster along with the best-fit linear trend line. Three clusters were used, one in right PTR (A), one in left PTR (B), and one in the posterior body of the corpus callosum (C).

total score across all domains. Future research can employ hypothesis-driven approaches such as fiber tractography to establish structure–function relationships between specific axonal pathways and sensory processing. Diffusion-based structural connectivity can also be combined with fMRI or MEG functional connectivity to provide multimodal imaging biomarkers for diagnosis, outcome prediction and monitoring interventions such as sensory processing and MSI training strategies. Using imaging and behavioral testing, we hope to move toward a more individualized model for understanding and treating children with sensory processing differences.

4.4. Summary and conclusion

Although sensory processing differences are well known to occur in association with other clinical conditions such as autism, there are individuals with behavioral sensory processing differences who do not meet the criteria for other known disorders. This study is the first to show that children affected with isolated sensory processing disorders have quantifiable differences in their brain structure. Despite likely etiologic heterogeneity and a small sample size, children with SPD show specific reduction in the white matter microstructure primarily affecting posterior cerebral tracts. Additionally, the reduced posterior white matter microstructural integrity in children with SPD correlates directly with the atypical sensory behavior. From a clinical perspective, these findings suggest that children with SPD have a specific imaging biomarker for their clinical disorder and the pattern of their shared structural difference (i.e. posterior decrease in white matter microstructural integrity) suggests that this disorder may be distinct from other overlapping clinical diagnoses, specifically attention deficit hyperactivity disorder and autism. This imaging biomarker not only presents an ideal diagnostic tool to be used in conjunction with other parent report and direct behavioral measures, but also informs treatments based on cognitive rehabilitation of the unimodal and multimodal sensory processing skills, such as directed occupational therapy, targeted computer training, and potentially brain stimulation.

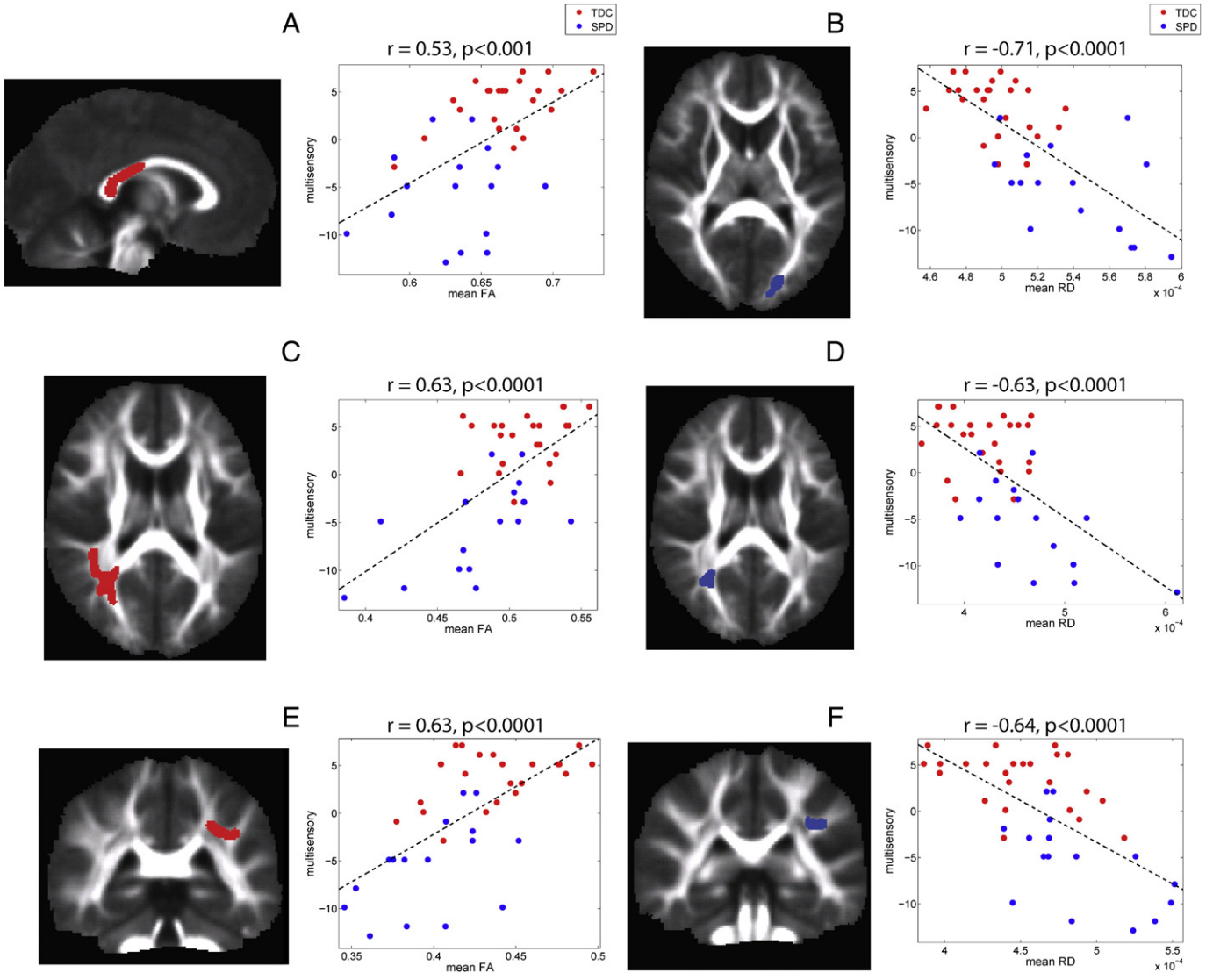

Fig. 4. Correlation of FA and RD with multisensory score: The left column displays the clusters extracted from the statistical image for the correlation ($p < 0.05$) and the right column displays the plot of mean FA in each cluster versus the mean-centered multisensory score for the TDC (red) and SPD (blue) groups. The correlation coefficient and corresponding p-value are provided for each cluster along with the best-fit linear trend line. Three clusters were used for both FA and RD. For FA, there was a cluster located in the posterior body and splenium of the corpus callosum (A), right PCR/SLF (C) and left SLF (E) and for RD, there was a cluster located in left optic radiation (B), the right PCR (D), and left SLF (F). Each cluster is displayed in red if the multisensory score is positively correlated with the DTI parameter and in blue if it is negatively correlated with the DTI parameter.

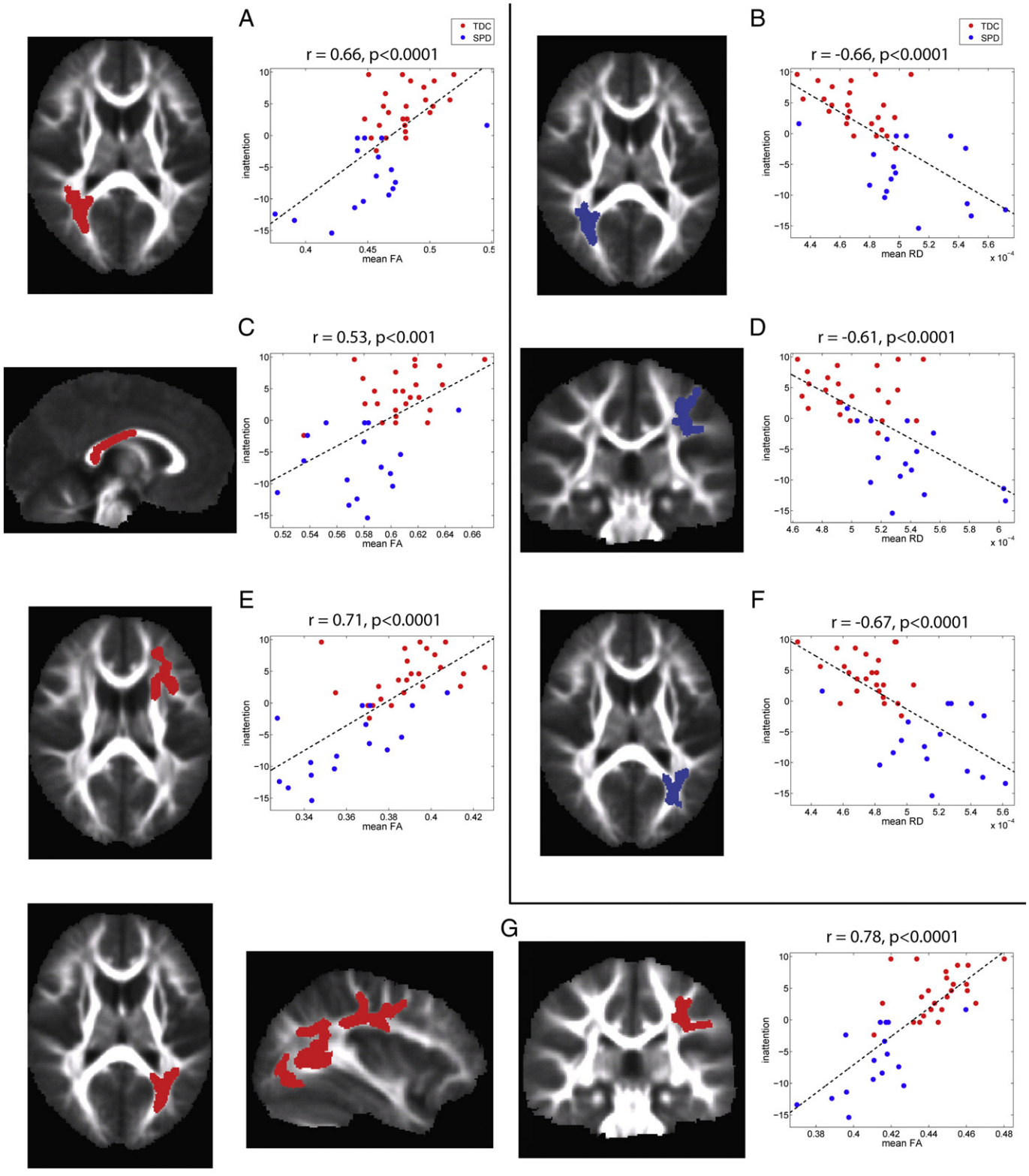

Fig. 5. Correlation of FA and RD with inattention score: The left column displays the clusters extracted from the statistical image for the correlation ($p < 0.05$) and the right column displays the plot of mean FA in each cluster versus the mean-centered inattention score for the TDC (red) and SPD (blue) groups. The correlation coefficient and corresponding p-value are provided for each cluster along with the best-fit linear trend line. The clusters used for FA were located in right PCR (A), the posterior body and splenium of the corpus callosum (C), left anterior corona radiata and ATR (E), and an extensive cluster encompassing left PTR and SLF (G). For RD, three clusters were used in bilateral PTR/PCR (B, F) and the left SLF (D). Each cluster is displayed in red if the inattention score is positively correlated with the DTI parameter and in blue if it is negatively correlated with the DTI parameter.

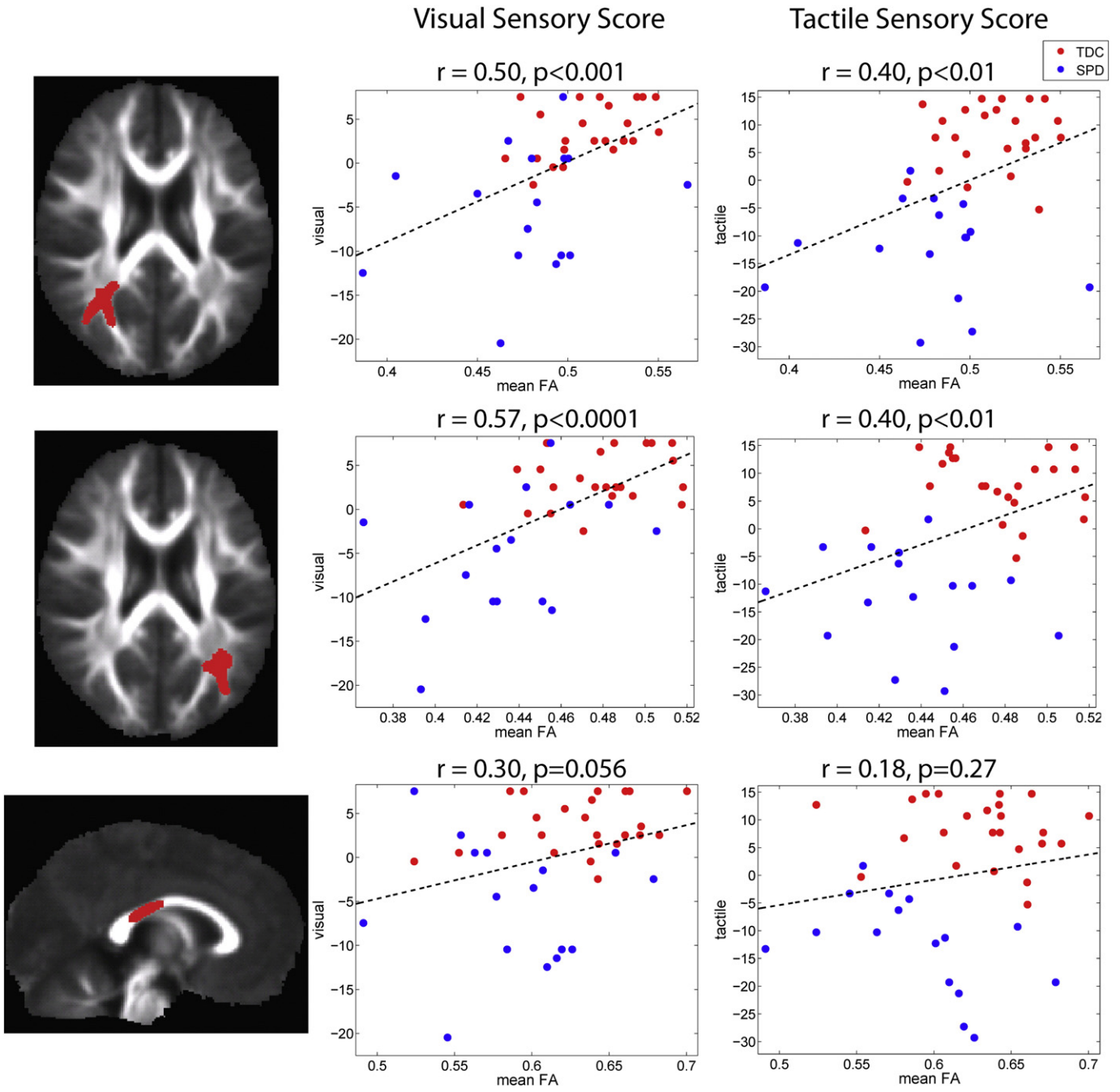

Fig. 6. Correlation of FA with tactile and visual sensory scores: The left column displays the clusters extracted from the statistical image for the correlation ($p < 0.05$) and the right column displays the plot of mean FA in each cluster versus the mean-centered visual and tactile scores for the TDC (red) and SPD (blue) groups. The correlation coefficient and corresponding p-value are provided for each cluster along with the best-fit linear trend line. The three clusters, one in right PTR (top row), one in left PTR (middle row), and one in the posterior body of the corpus callosum (bottom row) are identical to those in Fig. 3.

Acknowledgments

This work was funded by grants from the Wallace Research Foundation to E.J.M. and to P.M. J.P.O. and P.M. acknowledge support from the Simons Foundation. P.M. also acknowledges support from NIH R01 NS060776. E.J.M. has received support from NIH K23 MH083890.

References

Ahn, R.R., Miller, L.J., Milberger, S., McIntosh, D.N., 2004. Prevalence of parents' perceptions of sensory processing disorders among kindergarten children. American Journal of Occupational Therapy 58, 287–293.

Baranek, G.T., Roberts, J.E., David, F.J., Sideris, J., Mirrett, P.L., Hatton, D.D., Bailey Jr., D.B., 2008. Developmental trajectories and correlates of sensory processing in young boys with fragile X syndrome. Physical & Occupational Therapy in Pediatrics 28, 79–98.

Basser, P.J., Mattiello, J., LeBihan, D., 1994. MR diffusion tensor spectroscopy and imaging. Biophysical Journal 66, 259–267.

Beaulieu, C., 2002. The basis of anisotropic water diffusion in the nervous system — a technical review. NMR in Biomedicine 15, 435–455.

Ben-Sasson, A., Carter, A.S., Briggs-Gowan, M.J., 2009a. Sensory over-responsivity in elementary school: prevalence and social–emotional correlates. Journal of Abnormal Child Psychology 37, 705–716.

Ben-Sasson, A., Hen, L., Fluss, R., Cermak, S.A., Engel-Yeger, B., Gal, E., 2009b. A meta-analysis of sensory modulation symptoms in individuals with autism spectrum disorders. Journal of Autism and Developmental Disorders 39, 1–11.

Brett-Green, B.A., Miller, L.J., Gavin, W.J., Davies, P.L., 2008. Multisensory integration in children: a preliminary ERP study. Brain Research 1242, 283–290.
Brett-Green, B.A., Miller, L.J., Schoen, S.A., Nielsen, D.M., 2010. An exploratory event-related potential study of multisensory integration in sensory over-responsive children. Brain Research 1321, 67–77.
Bundy, A.C., Shia, S., Qi, L., Miller, L.J., 2007. How does sensory processing dysfunction affect play? American Journal of Occupational Therapy 61, 201–208.
Chait, M., de Cheveigné, A., Poeppel, D., Simon, J.Z., 2010. Neural dynamics of attending and ignoring in human auditory cortex. Neuropsychologia 48, 3262–3271.
Dunn, W., Westman, K., 1997. The sensory profile: the performance of a national sample of children without disabilities. American Journal of Occupational Therapy 51, 25–34.
Eaves, L.C., Wingert, H.D., Ho, H.H., Mickelson, E.C., 2006. Screening for autism spectrum disorders with the social communication questionnaire. Journal of Developmental and Behavioral Pediatrics 27 (Suppl. 2), S95–S103.
Fischl, B., 2012. FreeSurfer. NeuroImage 62, 774–781.
Goldsmith, H.H., Van Hulle, C.A., Arneson, C.L., Schreiber, J.E., Gernsbacher, M.A., 2006. A population-based twin study of parentally reported tactile and auditory defensiveness in young children. Journal of Abnormal Child Psychology 34, 393–407.
Hofer, S., Frahm, J., 2006. Topography of the human corpus callosum revisited? Comprehensive fiber tractography using diffusion tensor magnetic resonance imaging. NeuroImage 32, 989–994.
Huang, H., Zhang, J., Jiang, H., Wakana, S., Poetscher, L., Miller, M.I., van Zijl, P.C., Hillis, A.E., Wytik, R., Mori, S., 2005. DTI tractography based parcellation of white matter: application to the mid-sagittal morphology of corpus callosum. NeuroImage 26, 195–205.
Jenkinson, M., Bannister, P., Brady, M., Smith, S., 2002. Improved optimization for the robust and accurate linear registration and motion correction of brain images. NeuroImage 17, 825–841.
Leekam, S.R., Nieto, C., Libby, S.J., Wing, L., Gould, J., 2007. Describing the sensory abnormalities of children and adults with autism. Journal of Autism and Developmental Disorders 37, 894–910.
Liston, C., Cohen, M.M., Teslovich, T., Levenson, D., Casey, B.J., 2011. Atypical prefrontal connectivity in attention-deficit/hyperactivity disorder: pathway to disease or pathological end point? Biological Psychiatry 69, 1168–1177.
Lord, C., Rutter, M., Goode, S., et al., 1989. Autism diagnostic observation schedule: a standardized observation of communicative and social behavior. Journal of Autism and Developmental Disorders 19, 185–212.
Lord, C., Rutter, M., Le Couteur, A., 1994. Autism diagnostic interview-revised: a revised version of a diagnostic interview for caregivers of individuals with possible pervasive developmental disorders. Journal of Autism and Developmental Disorders 24, 659–685.
Mori, S., Crain, B.J., Chacko, V.P., van Zijl, P.C., 1999. Three-dimensional tracking of axonal projections in the brain by magnetic resonance imaging. Annals of Neurology 45, 265–269.
Mori, S., Wakana, S., van Zijl, P.C.M., 2005. MRI Atlas of Human White Matter. Elsevier.
Mori, S., Oishi, K., Jiang, H., et al., 2008. Stereotaxic white matter atlas based on diffusion tensor imaging in an ICBM template. NeuroImage 40, 570–582.
Mukherjee, P., McKinstry, R.C., 2006. Diffusion tensor imaging and tractography of human brain development. Neuroimaging Clinics of North America 16, 19–43.
Mukherjee, P., Miller, J.H., Shimony, J.S., et al., 2001. Normal brain maturation during childhood: developmental trends characterized with diffusion-tensor MR imaging. Radiology 221, 349–358.
Mukherjee, P., Miller, J.H., Shimony, J.S., et al., 2002. Diffusion-tensor MR imaging of gray and white matter development during normal human brain maturation. AJNR. American Journal of Neuroradiology 23, 1445–1456.
Mukherjee, P., Berman, J.I., Chung, S.W., Hess, C.P., Henry, R.G., 2008. Diffusion tensor MR imaging and fiber tractography: theoretic underpinnings. AJNR. American Journal of Neuroradiology 29, 632–641.
Smith, S.M., Nichols, T.E., 2009. Threshold-free cluster enhancement: addressing problems of smoothing, threshold dependence and localisation in cluster inference. NeuroImage 44, 83–98.
Smith, S.M., Jenkinson, M., Johansen-Berg, H., et al., 2006. Tract-based spatial statistics: voxelwise analysis of multi-subject diffusion data. NeuroImage 31, 1487–1505.
Tamm, L., Barnea-Goraly, N., Reiss, A.L., 2012. Diffusion tensor imaging reveals white matter abnormalities in attention-deficit/hyperactivity disorder. Psychiatry Research 202, 150–154.
Travers, B.G., Adluru, N., Ennis, C., et al., 2012. Diffusion tensor imaging in autism spectrum disorder: a review. Autism Research 5, 289–313.
Van Hulle, C.A., Schmidt, N.L., Goldsmith, H.H., 2012. Is sensory over-responsivity distinguishable from childhood behavior problems? A phenotypic and genetic analysis. Journal of Child Psychology and Psychiatry 53, 64–72.
Wechsler, D., 2003. WISC-IV: Administration and Scoring Manual. Psychological Corporation.
Wickremasinghe, A.C., Rogers, E.E., Johnson, B.C., Shen, A., Barkovich, A.J., Marco, E.J., 2013. Children born prematurely have atypical Sensory Profiles. Journal of Perinatology. http://dx.doi.org/10.1038/jp.2013.12 (Epub ahead of print Feb 14, 2013).
Yoshida, S., Oishi, K., Faria, A.V., Mori, S., 2013. Diffusion tensor imaging of normal brain development. Pediatric Radiology 43, 15–27.